

## The Risk of Solar Proton Events to Space Missions

Martin O. Burrell

NASA/Marshall Space Flight Center, Huntsville, Alabama

## SUMMARY

The total dose in rads-tissue from solar protons was tabulated for weekly time intervals, and the number of weeks which gave a dose above 25 rads behind 10 g/cm<sup>2</sup> of aluminum for the active 6 years of the 19th cycle were called dangerous or large event weeks. The number of such event weeks was found to be only 3 weeks for the past 20 years. Even though the chance for smaller events is examined, it was found that for any reasonable high confidence level (95%), the smaller events could be ignored. Consequently, the total particle flux for the 19th cycle was divided by a factor of 3 and determined a single large event week. Using this spectrum, the tissue dose in rads is calculated at the center of an aluminum spherical shell. To correct for geometric effects and self shielding, this dose may be reduced by a factor of about 3. To predict the probability of an event occurring, the Poisson distribution was the most logical choice. The confidence one can use in employing the Poisson process and arriving at confidence levels for the experimental value of the mean is investigated. Several examples are given for different mission lengths, and comparisons are made to other authors' results. An extension of the Poisson process is made to incorporate the concept of small sample theory and arrive at the expected distribution function which answers the following question. If  $x_0$  events are observed in time  $t_0$ , what is the probability of seeing  $x$  events in any observation time  $t$ ?

## INTRODUCTION

This study is concerned with the practical treatment of hazards from solar proton events outside the magnetosphere of the earth. It is not concerned with prediction of flares as such nor the long-range solar cycle indicators such as sun spots. The study of all solar proton events as such is only casually related to the problem of large dose rates inside realistic spacecraft. For example, in reference 1, there are 76 events listed from 1942 through 1963. Since 1963, there are probably an additional 24 more yielding a statistical sample of some 100 events. However, the correlation of this large sample with the events which are of real danger to space flight is very poor. For example, only 6 large events from 1950 to 1969 would have given about 85% of the total 20-year proton dose behind a thin wall of only 2 cm of aluminum. In addition, these 6 flares occurred in 3 weekly periods. Thus, 3 of these 6 large events occurred from July 10-16, 1959, 2 occurred from November 12-18, 1960, and on February 23, 1956, 1 large event was observed. The duration of an event is from 1 to 3 days. Even with this small sample, it seems that if conditions are suitable for a large event, the odds are very good that it will be followed within hours by another large event. Perhaps a time span of at least 1 week should be used to depict a total solar event, and it would be designated as the solar proton flux or dose per week. Under this definition, there are only 3 sample weeks of large solar events from about 1950 through 1969 (1,000 weeks). We are not dealing with an ordinary problem of statistical analysis, but with rare large events.

The reason that the writer has undertaken the awesome task of predicting the improbable is not by virtue of his background in solar physics or statistical analysis but because of his concern with protection of man and his radiation-sensitive equipment from space radiations for realistic spacecraft and missions. However, the reader should ask, why not leave this field of statistical astronomy to the experts. The answer is that the environmental scientists do not have to design or evaluate realistic shields for sensitive film or radiation-conscious astronauts.

The consequence of having several solar proton prediction models (which I do not wish to evaluate) has led to a wide disparity in results, especially when a reasonably high level of statistical certainty is desired. For example, at the 99% probability (percentile) level, the predicted dose behind 20 g/cm<sup>2</sup> of aluminum for a 1-year mission may vary by a factor of 10 or more between different writers<sup>[2]</sup>. Now this may not sound too bad considering the nature of the problem, but if a mission is planned with the requirement that the astronauts should not receive doses exceeding 100 rads skin dose with a 99% probability, and if one solar proton dose prediction model requires a shield of only 15 g/cm<sup>2</sup> and another model 50 g/cm<sup>2</sup>, the radiation analyst has to make a vital decision, possibly affecting the life of an astronaut. Since no one wishes to be responsible for making a decision which could lead to dire consequences, the most pessimistic model is often chosen. This writer would not question this approach except that the desire to be on the safe side may readily get out of hand with the subsequent loss in mission capability.

## A PRIMITIVE DOSE MODEL IS PROPOSED

The most direct measure of the hazard of a given solar proton event is the rads (.01 J/Kg) - tissue absorbed dose that would be measured behind various thicknesses of a typical spacecraft material such as aluminum. The simplest method is to find the point tissue dose at the center of a spherical shell of aluminum. However, due to self shielding by the astronaut (approximately a factor of 2) and spacecraft geometry as well as on-board equipment, the actual skin dose may be less by a factor of 3 or more than the point dose at the center of a spherical shell. This factor varies depending on the solar proton spectrum, the spacecraft geometry, and the location of the astronaut in the craft. This writer suggests using a factor of about 3 reduction for the solar proton point dose at the center of a spherical shell in order to estimate the likely skin dose to an astronaut in a real spacecraft of a given average thickness. (It

should be noted that this factor of 3 may be too large for a very "hard" spectrum such as seen in the trapped radiation belts, when a factor of 2.5 may be more in order.) To correct for depth dose (bone-marrow depth), a thickness of 5 cm of tissue is often employed. This is approximately equal to 6.5 g/cm<sup>2</sup> of aluminum in equivalent shielding effectiveness.

In order to clarify the exact assumptions which are to be employed, the following information is pertinent. The only adequate data available at this writing for solar proton predictions are from the 19th cycle (1954-64). However, there have been observations of sun spots (indicator of solar activity) for about 200 years. Based on 200+ years of observations, where the first cycle would date back to the middle of the 18th century (average cycle length is about 11 years), the 19th cycle had the highest maximum sun spot count yet recorded. In fact the average maximum sun spot count is more than a factor of 2 lower. The 20th cycle, which we are now well into (past the peak activity), has a sun spot count somewhat above this average. There has not been a large solar proton event comparable to the eight largest events of the 19th cycle (dose behind 10 g/cm<sup>2</sup>). At this point, one may be led to believe that the 19th cycle is a fairly rare type cycle. With the present low occurrence of large solar proton events and the rather extensive sun spot counting dating back over 200 years, one might conclude that the probability of getting a solar cycle as active as the 19th is on the order of 1/20 or 0.05. This, of course, cannot be objectively demonstrated, and will not be, unless considerably more knowledge is obtained about the physics of the sun. One valid objection to the above is that the sun spot number is a poor indicator of large solar proton events. Also, the sun spot indicator may have changed during the last 50 years due to better observations, so that possibly the first 15 of the 20 observed cycles should not be used. The purpose of this paper is not to attempt to evaluate the above but to present the information for the reader's consideration. At any rate the reader may not find it difficult to believe that the use of the 19th cycle solar proton flux data may yield a pessimistic estimate of the solar proton hazard. With the above background, we can at least study the proton events characterized by the 19th cycle and infer proton events for future cycles similar to the 19th cycle.

Next we consider the observation that during the 19th cycle, the large solar proton events did occur on the whole around the most active years of the 11-year cycle, however not necessarily in proportion to sun spot count. It is generally assumed that there were only about 6 years of observed large solar proton events. Thus the following analysis is based on the so-called active 6 years (300 weeks) of the cycle. The second assumption is that it is fair and logical to lump the actual dose rates over an active week into units of total dose per week (see Introduction). This may include up to 3 proton events in a given week. Thus, instead of dealing with fundamental units of proton events, we propose to deal with observed weekly dose rates behind various aluminum thicknesses. The data available from various sources gave a total of 24 proton events worth considering. (The 30 or more events discarded gave less than 3 rads total behind 5 g/

cm<sup>2</sup> of aluminum). The results of grouping this data into weekly time periods gave a total of 18 weeks with the frequencies of 13 weeks having 1 event, 4 weeks having 2 events, and 1 week having 3 events. Most of this data is recorded in NASA TND 4404 [3] on pages 16-23. The only major revision in reference 3 is in the use of the spectrum of A. J. Masley[4] for the November 12, 1960, flare.

One note of explanation should be made regarding the dose rates which are used in this study. They include a correction for secondary particles and thus are the sum of the primary proton dose and the secondary particles (neutrons and protons). This total dose at 20 g/cm<sup>2</sup> is about 20% and at 10 g/cm<sup>2</sup> about 10% above the primary proton dose rates.

Now we come to a very treacherous part of the analysis. How do we choose a rational and sufficient model for an event dose-week for solar protons? Table 1 is presented as a summary of the weekly solar proton doses of the 19th solar cycle which the writer will consider. The absorbed doses in rads-tissue were calculated at the center point of a spherical shell of aluminum with the shell thickness being designated as the shield.

TABLE 1: WEEKLY DOSES OF THE 19TH SOLAR CYCLE

Sample Number	Week	Year	Number of Flares	Shield (6-Year Dose)			Remarks
				5(90G) <sup>a</sup>	10(251)	20(73)	
1	Nov 12 - 18	1960	2	456	83.4	17.0	Category 1 - Large Weekly Doses $\lambda_1$ 0.01
2	July 10 - 16	1959	3	216	75.0	21.2	
3	Feb. 23	1956	1	92	50.0	24.8	
	Summed Dose Percent of Total 6-Year Dose		(6)	764	208.4	63.0	Approximately 85 Percent of 6-Year Total
				84.3	53	86.3	
1	May 10	1959	1	59.3	18.3	4.4	Category 2 - Medium Weekly Doses $\lambda_2$ 0.02
2	July 18 - 20	1961	2	22.0	8.2	2.4	
3	March 23	1958	1	10.9	2.5	0.4	
4	July 7	1958	1	10.5	2.3	0.4	
5	Jan. 20	1957	1	8.3	1.8	0.3	
6	Oct. 20	1957	1	4.1	1.8	0.7	
	Summed Dose Percent of Total 6-Year Dose		(7)	115.1	34.9	8.6	Approximately 13 Percent of 6-Year Total
				12.7	13.9	11.8	
1	Aug. 22 - 26	1958	2	5.9	1.0	0.2	Category 3 - Small Weekly Doses $\lambda_3$ 0.03
2	Aug. 29	1957	1	4.2	0.8	0.1	
3	Nov. 20	1960	1	3.6	1.5	0.05	
4	Aug. 3	1956	1	2.2	1.0	0.4	
5	Sept. 13	1960	1	2.9	1.2	0.5	
6	Aug. 10	1958	1	1.8	0.4	0.1	
7	July 3	1957	1	1.2	0.43	0.03	
8	July 12	1961	1	1.4	0.39	0.04	
9	April 28 - 29	1960	2	0.77	0.27	0	
	Summed Dose Percent of Total 6-Year Dose		(11)	23.97	6.90	1.42	Approximately 2 Percent of 6-Year Total
				2.65	2.73	1.95	

a. The first number is the shield thickness in g/cm<sup>2</sup>-aluminum, the number in parenthesis is the 6-year dose behind the shield.

The data of Table 1 have been grouped into three categories: (1) large weekly doses, (2) medium weekly doses, and (3) small weekly doses.

Category (1), consisting of only 3 weeks, gave more than 84% of the total 6-year dose. Category (2), with 6 samples, gave about 13%, and Category (3), with 9 samples, gave less than 3% of the total dose.

The grouping which is shown is certainly not unique, and the last 2 weeks of Category (2) perhaps should be in Category (3), or perhaps the largest dose week of Category (2) should be in Category (1). The following work has attempted to provide for various combinations which the reader may wish to investigate by making the methods of approach more important than the choice of a precise set of data.

Since over 84% of the total solar proton dose is grouped into the 3 weeks of the first category, it would seem that one feasible solar proton dose model for an active week could be depicted by dividing the total 6-year dose behind the various shields by 3. Since the most active phase of the 19th cycle is about 6 years, it seems sufficient to use 300 weeks as the basic period of major solar activity. With this assumption, which will be used throughout this study, it follows that the estimated weekly expectation of a dangerous large solar proton dose would be  $\lambda_0 = .01$  (event/week).

In any case, the chance for an event of Category (2) or Category (3) is more likely to occur than one of Category (1) for a short exposure time. For this reason, a model will also be developed to reflect medium and small flare doses as well as large events. Thus, two solar proton dose models will be constructed and results compared in the following work.

The next part of our approach is to choose the best composite 19th cycle solar proton flare data which is available and arrive at total tissue dose in rads from primary and secondary particles at the center of spherical shells with varying thicknesses. T. T. White, et. al.<sup>[6]</sup> have developed a composite model (MSC model) for the total proton flux during the 19th cycle. This model gives a larger dose for energies less than about 115 MeV than a model based on Webber's work<sup>[5]</sup>. Above 115 MeV, a composite flare model based on Webber's work (to be designated as the MSFC model) gives a larger dose. The 19th cycle composite 6-year proton spectrum which will be used in this work is the following:

$$\text{(MSC) I. } J(>p) = 5.28 \times 10^{11} e^{-p/73} \quad (30 \leq E \leq 115 \text{ MeV}) \quad (1)$$

$$\text{(MSFC) II. } J(>p) = 1.14 \times 10^{11} e^{-p/200} \quad (E > 115 \text{ MeV}),$$

where  $p$  is the rigidity units of MV and  $J(>p)$  is the integral spectra (proton/cm<sup>2</sup>) with energies above  $p$ . For protons, the relationship between  $p$ (MV) and  $E$ (MeV) is given by  $p = \sqrt{E^2 + 1876E}$  (ref. 3, page 15).

Using the spectrum above, the best estimate of the 6-year (300 weeks) total dose (primaries and secondaries) is given in Fig. 1. From Fig. 1 and Table 1, the solar proton one-week-dose event models are constructed (Fig. 1 gives the magnitude, and Table 1 gives the fractions). Model I will be the dangerous solar event model which is represented by 3 large events over a period of 300 weeks.

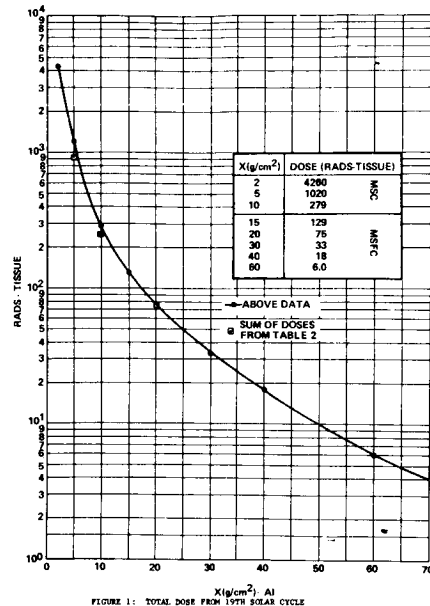


FIGURE 1: TOTAL DOSE FROM 19TH SOLAR CYCLE

The expected number of events in 1 week is given by  $\lambda_0 = .01$  (event/week). Model II will depict the possibility of a large, medium, or small dose in a week where the percentages of the total dose in Table 2 are used to determine the relative size of a dose week in the three groups. For the three categories of Table 1, the values  $\lambda_1 = .01$ ,  $\lambda_2 = .02$ , and  $\lambda_3 = .03$  are the mutually independent weekly expectations of large, medium, and small doses, respectively. Table 2 summarizes the dose models. It should be clear that the writer has presented in Table 2 only the primitive elements of a probability model. Thus the table gives the small sample estimates of the weekly expectations ( $\lambda$ ) and the consequences (rads/week) if an event occurs according to Model I or II. It should also be made clear that the values of  $\lambda$  are valid only for the 300 most active weeks of a solar cycle similar to the 19th. The major unknown factor is an estimate of the chance of obtaining a solar cycle that would give total proton doses as large or larger than the 19th cycle.

The values of  $\lambda$  should be smaller for the so-called quiet sun (260 weeks) or else the magnitude of an event reduced to one of Category (3). Perhaps one might assume that  $\lambda = .02$  (one event per year) during the 260 weeks of the quiet sun, but an event should be depicted by the D<sub>3</sub> column (small event) of Model II.

As a final conclusion to this section, it is of interest to recall that Fig. 1 represents the total dose versus spherical shell thickness for the 19th cycle. If for the data of Fig. 1 as described above, an effort is made to correct for the self shielding of an astronaut and the complex geometry of a spacecraft which has aluminum walls of 13.5 g/cm<sup>2</sup> (assume that a 5 cm depth dose corresponds to an additional aluminum thickness of 6.5 g/cm<sup>2</sup>) then the 5 cm depth dose is estimated by dividing the dose at 20 g/cm<sup>2</sup> by a factor of 3. Thus one finds that the total dose from the 19th cycle was 25 rads at 5 cm tissue depth. Of course, this value is for the solar proton dose and does not account for the galactic cosmic ray dose which may range from 5 to 12 rads per year behind 20 g/cm<sup>2</sup> depending on how much dose is contributed by the

heavy cosmic ray particles ( $Z > 2$ ). The implications of all the above are simply that since the 19th solar cycle was an example of a very active sun, and if one believes that the high energy proton fluxes received during this cycle are associated with this activity, he must be cautious in drawing certain conclusions. For example, the same astronaut above may have received from 30 to 70 rads from galactic cosmic rays during a 6-year trip whereas the above dose from solar protons at bone marrow depth was 25 rads ( $13.5 \text{ g/cm}^2 - \text{al. walls}$ ). Here one assumes that the galactic cosmic ray spectrum is so energetic that geometry factors are negligible for dose reduction. Thus the cosmic ray dose component may determine the limiting dose factor for long duration space travel. The purpose of the foregoing is not to minimize the importance of solar proton events but to point out that it may be quite feasible to shield against solar protons but probably impractical to consider shielding against galactic cosmic rays, and this very fact may be more important in determining man's exposure time to space outside the earth's magnetic field than the solar protons.

#### A PROBABILITY MODEL IS DERIVED

In this section, we shall address ourselves to the problem of choosing and using a probability density function in order to arrive at the probability of getting "x" events in "t" weeks and the associated problem of probability or percentile levels. The important question of establishing confidence intervals for the basic statistical parameters which are obtained from a small sample will be undertaken in the next section. In this section, we will be making the naive assumption that the basic statistics or population parameters (mean and variance) are well known, either by experience or apriori knowledge.

In order to derive the probability model, which seems to be the most natural outgrowth of the solar proton dose week, the process will be described in terms of probabilities  $P_n(t)$  that exactly n events occur during a time interval t (weeks in our case). Thus,  $P_0(t)$  is the probability of no event in the interval t and  $1 - P_0(t)$  is the probability of one or more events. Next we define  $\lambda$  to be the mean or expectation of an event for a unit time interval. That is,

$$\hat{\lambda} = \frac{\text{no. of events}}{\text{total weeks of observation}} \quad (2)$$

is a statistical estimate of  $\lambda$ . More precisely,  $\lambda$  is a constant which determines the density of points on the t axis. Thus for a small interval of time  $\Delta t$  the probability of one or more events is given by:

$$1 - P_0(\Delta t) = \lambda \Delta t + \epsilon(\Delta t), \quad (3)$$

where  $\epsilon(\Delta t)$  is an infinitesimal and small compared to  $\lambda \Delta t$  such that

$$\lim_{\Delta t \rightarrow 0} \frac{\epsilon(\Delta t)}{\Delta t} = 0 \quad (3a)$$

Now we make the following postulate:

Whatever the number of events during (0,t) the probability during (t, t +  $\Delta t$ ) that one event occurs is given by  $P_1(\Delta t) = \lambda \Delta t + \epsilon_0(\Delta t)$ , and the

probability that more than one event occurs is given by  $P_{n>1}(\Delta t) = \epsilon_1(\Delta t)$ .

These conditions are the basic assumptions of the Poisson process (Feller[7], pages 400-402). It should be clear that we are stating that for a small time interval  $\Delta t$ , the chance for one event is approximately  $\lambda \Delta t$ , and the chance for more than one event is very small compared to  $\lambda \Delta t$ . Since t is for a relative time scale, it is not contradictory that  $\Delta t$  of 1 week can be small on our time scale. The above conditions lead to a system of differential equations for  $P_n(t)$ . They are:

$$dP_n(t)/dt = -\lambda P_n(t) + \lambda P_{n-1}, \quad n \geq 1, \quad (4)$$

and

$$dP_0(t)/dt = -\lambda P_0(t), \quad n = 0. \quad (5)$$

From Equation (5) and  $P_0(0) = 1$ , we get:

$$P_0(t) = e^{-\lambda t}. \quad (6)$$

Using Equation (6) and  $P_1(0) = 0$ , Equation (4) can be solved for  $P_1(t) = \lambda t e^{-\lambda t}$ . Using the fact that  $P_n(0) = 0$ , ( $n > 0$ ), Equation (4) becomes a recursion equation and successive values of  $P_n(t)$  can be found. The resulting solutions give the terms of the Poisson distribution:

$$P_n(t) = e^{-\lambda t} \frac{(\lambda t)^n}{n!}. \quad (7)$$

If the reader accepts the postulate following Equation (3), the Poisson distribution is the natural outcome. The foregoing arguments have been presented in order to minimize the illusion that the author has pulled a distribution function out of the sky. For a more rigorous treatment, reference 7 is recommended.

There are many interesting uses of the Poisson distribution in addition to the occurrence of rare events in a continuum of time. The distribution is used to approximate the binomial distribution for the case of rare events ( $p < .05$ ). The word rare means individually rare. In a large population, several such events may occur, but the probability of occurrence of each individual event is small. For example, the number of people killed by horses in 1969. An important feature of the Poisson distribution is that for large values of the mean ( $\lambda t \gg 20$ ), the distribution approaches the normal (or Gaussian) distribution. There are many applications of the Poisson distribution given in any standard text on probability and statistics. The most common include such studies as the number born blind in a large city, radioactive disintegration, bacteria on plates, telephone traffic, etc. The remainder of this section will be devoted to a discussion of the Poisson distribution and how to apply it to our class of problems.

If a discrete variable x has a Poisson distribution, then the probability that  $[X = x]$  is given by the expression:

$$P[X = x] = \frac{e^{-m} m^x}{x!}, \quad x = 0, 1, 2, \dots, \quad (8)$$

and  $P[X = 0] = e^{-m}$ , since  $0! = 1$ .

The mean (or expected value of the variable  $x$ ) is given by  $\mu = m$ , the variance  $\sigma^2$  is given by  $\sigma^2 = m$ , and the standard deviation is simply given by  $\sigma = \sqrt{m}$ . The summation equation,

$$\sum_{x=0}^{\infty} e^{-m} m^x / x! = 1, \quad (8a)$$

is satisfied. Since we are primarily interested in the time-dependent form of the Poisson,  $m = \lambda t$  becomes the mean. Even though the Poisson is discrete in the variable  $x$ , it is continuous in  $t$ . For our purpose, we shall write the Poisson distribution as:

$$P[X = x] = \frac{e^{-\lambda t} (\lambda t)^x}{x!}, \quad x = 0, 1, 2, \dots, \quad (9)$$

where  $t$  = number of weeks,  $x$  = number of events in  $t$  weeks,  $\lambda$  = mean number of events per week with  $(\lambda t)$  becoming the expected or mean number of events in  $t$  weeks, and  $P[X = x]$  is the probability of exactly  $x$  events in  $t$  weeks.

If one wished to find a value of  $x$  which would not be exceeded say at least 99% of the time (1% chance at most of exceeding  $x$ ) for a given  $\lambda t$ , the accumulative distribution function  $P[X \leq x^*]$  is utilized. The value of  $x$  which we seek is the smallest  $x^*$  which satisfies

$$\Pr[X \leq x^*] = \sum_{x=0}^{x^*} \frac{e^{-\lambda t} (\lambda t)^x}{x!} \geq P, \quad (10)$$

where  $P = .99$  for the case in question.

Since we are dealing with a discrete distribution function, the inequality is necessary, and one usually obtains a value of  $x^*$  which corresponds to a value slightly above  $P$  (.99). This discrepancy is usually circumvented by the proper use of the words "at least" and "at most."

Next, we will examine how to apply the above information to our problem of predicting the solar proton dose that would be seen on a space mission at various percentile levels. For simplicity, let us assume that if an event occurs, it is depicted by the so-called "large" event model or Model I of Table 2. Using this model, the sample statistical estimate of  $\lambda_0 = .01$  event/week, and for convenience, assume the duration of exposure to large solar events is 100 weeks, then the value of  $\lambda t = 1.0$  for the Poisson distribution. Now assume that we wish to find the dose levels that would be exceeded 27%, 2%, and 0.1% of the time. Applying Equation (10) with  $P$  taking on the values 0.73, 0.98, and 0.999, we see that the values of  $x$  are 1, 3, and 5 events. So to find the dose at the respective levels, we multiply the doses behind the various shield thicknesses of Model I by the values of  $x$  above. The results are plotted in Fig. 2. Note that the 73.6% level corresponds in our model to the mean or expected value of the Poisson distribution. The percentile level at the expected value is found only when  $\lambda t$  is an integer. It becomes smaller approaching 50% as  $\lambda t$  increases to large values. For example, when  $\lambda t = 20$ , the percentile at  $x^* = 20$  is 55.9%.

A similar computation can be carried out using event Model II. The values of the Poisson mean become respectively  $\lambda_1 t = 1.0$ ,  $\lambda_2 t = 2.0$ , and  $\lambda_3 t = 3.0$  where  $t = 100$  weeks. Tables are constructed, and the following results are found at the expected value, 98% and 99.9% level. For the

TABLE 2: MODELS OF A ONE-WEEK DOSE EVENT FOR THE ACTIVE 300 WEEKS OF THE 19TH SOLAR CYCLE

MODEL I		MODEL II			
$X(g/cm^2)$	$N = 3^*$ 100% $\lambda_0 = .01^\dagger$	$N(\text{Large})=3$ 84% $\lambda_1 = .01$	$N(\text{Med.})=6$ 13% $\lambda_2 = .02$	$N(\text{Small})=9$ 3% $\lambda_3 = .03$	$\sum_{i=1}^3 \lambda_i D_i$
$D_0$ (Rads/Weeks)		$D_1$ (Rads/Week)	$D_2$ (Rads/Week)	$D_3$ (Rads/Week)	Total Dose 300 Weeks
2	1420	1195	95	15	4290
5	340	286	24	3.4	1032.6
10	93	78	7.5	0.9	281.1
15	43	36	3.5	0.43	132.87
20	25	21	2.0	0.25	77.25
30	11	9.3	0.80	0.11	33.69
40	6	5.03	0.45	0.06	18.33
60	2	1.70	0.15	0.02	6.18

\* The  $N$  indicates the number of weeks used in dose category.

\*\* The  $\Sigma$  gives the percent of total dose in the category.

† The " $\lambda$ " gives the expectations (probability) of category for one week.

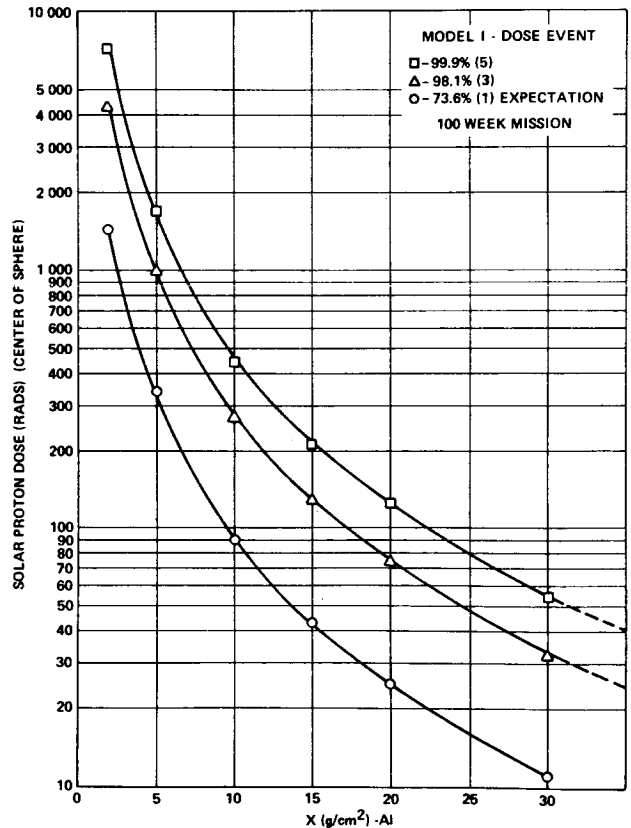


FIGURE 2: PROTON DOSE FOR 100-WEEK MISSION

large events,  $x = 1, 3,$  and  $5$ ; for the medium events,  $x = 2, 5,$  and  $8$ ; and for the small events,  $x = 3, 7,$  and  $10$ . The percentile values at the expected or mean value levels ( $x^* = \lambda t$ ) are 73.6%, 67.7%, and 64.7%, respectively. In order to reduce the necessity of repetition, this set of levels could be denoted as approximately 70% level. The comparison of results from these totals to Fig. 2[8] indicate very good agreement. A useful rule would be: Empirical Rule - If at a given probability level there is at least one large event, then Model I is sufficient to describe the radiation hazard. If no large event is found at the given probability level, then Model II should be used.

At this point, it might be useful to depict several curves similar to Fig. 2 for various mission times  $t$ , with  $\lambda = .01$  event/week, at given probability or percentile levels. In order to do this, arrays could be constructed for various values of  $\lambda t$ , and the number of events,  $x$ , necessary to satisfy the inequality of Equation (10) could be found for various values of  $P < 1$ .

Rather than provide a multitude of similar graphs, Table 3 will allow the reader to find the number of events for a range of anticipated values of  $\lambda t$  at 9 different percentile levels from 50 to 99.9%. Table 3 was constructed by choosing a probability level,  $P$ , the number of events,  $N$ , and then finding the value of  $m(-\lambda t)$  that satisfied the following equation:

$$\Pr(x \leq N) = \sum_{x=0}^N \frac{e^{-m} m^x}{x!} = P, \quad (m = \lambda t) \quad (11)$$

TABLE 3: VALUES OF  $\lambda t$  TO SATISFY  $\Pr(x \leq N) = P$

N	P	0.001	0.005	0.010	0.025	0.050	0.100	0.15	0.25	0.50
		99.9 Percent	99.5 Percent	99.0 Percent	97.5 Percent	95.0 Percent	90.0 Percent	85.0 Percent	75.0 Percent	50.0 Percent
0	0.0010	0.0050	0.010	0.025	0.051	0.105	0.16	0.29	0.69	
1	0.045	0.10	0.15	0.24	0.36	0.53	0.68	0.96	1.68	
2	0.19	0.34	0.44	0.62	0.82	1.10	1.33	1.73	2.67	
3	0.43	0.67	0.82	1.09	1.37	1.74	2.04	2.54	3.67	
4	0.74	1.06	1.28	1.62	1.97	2.43	2.79	3.37	4.67	
5	1.11	1.54	1.79	2.20	2.61	3.15	3.56	4.22	5.67	
6	1.52	2.04	2.33	2.81	3.29	3.89	4.35	5.08	6.67	
7	1.97	2.57	2.91	3.45	3.98	4.66	5.15	5.96	7.67	
8	2.45	3.13	3.51	4.12	4.70	5.43	5.97	6.84	8.67	
9	2.95	3.72	4.13	4.80	5.43	6.22	6.80	7.73	9.67	
10	3.48	4.32	4.77	5.49	6.17	7.02	7.64	8.62	10.67	
11	4.04	4.94	5.43	6.20	6.92	7.83	8.48	9.52	11.67	
12	4.61	5.58	6.10	6.92	7.69	8.65	9.34	10.42	12.67	
13	5.20	6.23	6.78	7.65	8.46	9.47	10.19	11.33	13.67	
14	5.79	6.89	7.48	8.40	9.25	10.30	11.06	12.24	14.67	
15	6.41	7.57	8.18	9.15	10.04	11.14	11.92	13.15	15.67	
16	7.03	8.25	8.89	9.90	10.83	11.98	12.79	14.07	16.67	
17	7.66	8.94	9.62	10.67	11.63	12.82	13.67	14.99	17.67	
18	8.31	9.64	10.35	11.44	12.44	13.67	14.55	15.91	18.67	
19	8.96	10.35	11.08	12.22	13.25	14.53	15.43	16.83	19.67	
20	9.62	11.07	11.83	13.00	14.07	15.38	16.31	17.75	20.67	
21	10.29	11.79	12.57	13.79	14.89	16.24	17.20	18.68	21.67	
22	10.96	12.52	13.33	14.58	15.72	17.11	18.08	19.61	22.67	
23	11.65	13.26	14.09	15.38	16.55	17.97	18.98	20.54	23.67	
24	12.34	14.00	14.85	16.18	17.38	18.84	19.88	21.47	24.67	
25	13.03	14.74	15.62	16.98	18.22	19.72	20.77	22.40	25.67	
26	13.73	15.49	16.40	17.79	19.06	20.59	21.67	23.34	26.67	
27	14.44	16.25	17.17	18.61	19.90	21.47	22.57	24.27	27.67	
28	15.15	17.00	17.96	19.42	20.75	22.35	23.48	25.21	28.67	
29	15.87	17.77	18.74	20.24	21.59	23.23	24.38	26.15	29.67	
30	16.59	18.53	19.53	21.06	22.44	24.11	25.28	27.09	30.67	
31	17.32	19.30	20.32	21.89	23.30	25.00	26.19	28.03	31.67	
32	18.05	20.08	21.12	22.72	24.15	25.89	27.10	28.97	32.67	
33	18.78	20.86	21.92	23.55	25.01	26.77	28.01	29.91	33.67	
34	19.52	21.64	22.72	24.38	25.87	27.66	28.92	30.85	34.67	
35	20.26	22.42	23.53	25.21	26.73	28.56	29.83	31.79	35.67	
36	21.00	23.21	24.33	26.05	27.59	29.45	30.75	32.74	36.67	
37	21.76	24.00	25.14	26.89	28.46	30.34	31.66	33.68	37.67	
38	22.51	24.79	25.96	27.73	29.33	31.24	32.58	34.63	38.67	
39	23.26	25.59	26.77	28.58	30.20	32.14	33.50	35.57	39.67	
40	24.02	26.38	27.59	29.42	31.07	33.04	34.42	36.52	40.67	

a.  $P = 1 - \alpha$   
b. If  $\lambda t$  lies between two entries, use  $N$  corresponding to the largest entry. Thus, if  $\lambda t = 0.5$ , use  $N = 4$  at the 95.0-percent level. If  $\lambda t$  is less than or equal to the top entry, use  $N = 0$ . Thus, if  $\lambda t = 0.02$ ,  $N = 0$  at the 97.5-percent level, but  $N = 1$  at the 99.0-percent level.

The values of  $m = \lambda t$ , found in this manner, is the expected value or mean of the Poisson distribution which has a percentile level of exactly  $P \times 100\%$  for  $N$  or less events.

The top of Table 3 is headed with a row of values labeled  $\alpha$  which denotes the probability of more than  $N$  events or simple  $\alpha = 1 - P$ . The probability statements using  $\alpha$  will be made as follows: the probability is no greater than  $\alpha$  that more than  $N$  events will be observed in  $t$  weeks. The use of  $\alpha$  probabilities will be derived in the next section. The range of values in Table 3 should provide for the refinements needed in the following work.

CONFIDENCE INTERVALS ARE ESTABLISHED

The results of the previous section depended strongly on the choice of the parameter  $\lambda$  or the probability of having a large event week. In this section, we will establish the confidence we can place on the value of  $\lambda$  as calculated from observed sample data. One of the virtues of the Poisson distribution is that the value of the mean ( $m = \lambda t$ ) completely determines the distribution function; i.e.,  $\sigma^2 = m$ , whereas the mean and variance ( $\sigma^2$ ) is needed for most distribution functions, and they are not simply related. Thus in dealing with small sampling statistics from a normal distribution, one needs to establish confidence intervals for both the mean and the variance.

In order to more clearly explain the intent of this section, an example will be given. The Poisson law arises very often in certain biological problems such as organisms distributed at random over the bottom of a lake. The number of such organisms found in a series of trial dredgings from separate small areas of the same size will follow this law. Statisticians calculate boundaries of possible outcomes from a given small sample, and these values are called confidence limits at a certain probability level for the assumed distribution function. Now, if a biologist counted 21 organisms from one of his dredgings, he could assert that he is 95% confident that the mean or expected value lies between 13 and 32 organisms per unit area assuming a Poisson distribution. Thus with only one sample and assumption of a Poisson process, it is possible to set upper and lower bounds on possible outcomes at a given probability level. From the above example, we can assert that if many dredgings are made, we expect only 5% will contain a number of organisms outside the predicted range.

Returning to the basic problem, we wish to establish the confidence interval on  $m$ , hence to find the probability

$$\Pr(m'' \leq m \leq m') \geq (1 - 2\beta) 100\% \quad (12)$$

where  $1 - P = \beta$ .

Now if  $P = .99$  and  $\beta = .01$ , then

$$\Pr(m'' \leq m \leq m') \geq 98\% \quad (12a)$$

and we are at least 98% sure that  $m$  lies between  $m'$  and  $m''$ , where  $m$  has only a 1% chance of being greater than  $m'$ . We can now write the general set of equations which will determine the value of  $m'$  and  $m''$ :

$$\sum_{x=0}^{x_0} \frac{e^{-m'} (m')^x}{x!} = 1 - P = \beta, \quad (13)$$

and

$$\sum_{x=x_0}^{\infty} \frac{e^{-m''} (m'')^x}{x!} = \beta, \quad (14)$$

or

$$\sum_{x=0}^{x_0-1} \frac{e^{-m''} (m'')^x}{x!} = 1 - \beta, \quad (15)$$

where  $x_0$  is observed number of events. The form of the above equation is an outgrowth of using a discrete distribution function and follows the common practice in textbooks on statistics. Solving Equations (13) and (15) for  $m'$  and  $m''$  by use of Newton's method, the upper and lower bounds on  $m$  are found for " $x_0$ " observed events. Table 4 summarizes these results for 8 different values of  $\beta$  or  $P$ . Fig. 3 depicts a typical result taken from Table 4.

TABLE 4: UPPER AND LOWER BOUNDS FOR THE MEAN AT PROBABILITY OF  $P = (1 - \beta)100\%$

Confidence Interval	99.8 Percent		99.0 Percent		98.0 Percent		95.0 Percent	
	$\beta$ 0.001		0.005		0.010		0.025	
Events, $x_0$	Lower Bound	Upper Bound	Lower Bound	Upper Bound	Lower Bound	Upper Bound	Lower Bound	Upper Bound
0	0	6.91	0	5.30	0	4.61	0	3.69
1	0.001	9.23	0.005	7.43	0.01	6.64	0.025	5.57
2	0.045	11.23	0.10	9.27	0.15	8.41	0.24	7.22
3	0.19	13.06	0.34	10.98	0.44	10.05	0.62	8.77
4	0.43	14.79	0.67	12.59	0.82	11.60	1.09	10.24
5	0.74	16.45	1.04	14.15	1.28	13.11	1.62	11.67
6	1.11	18.06	1.54	15.66	1.79	14.57	2.20	13.06
7	1.52	19.63	2.04	17.13	2.35	16.00	2.81	14.49
8	1.97	21.16	2.57	18.58	2.97	17.40	3.45	15.78
9	2.45	22.66	3.13	20.00	3.51	18.78	4.12	17.08
10	2.96	24.13	3.72	21.40	4.13	20.14	4.80	18.39
11	3.49	25.59	4.32	22.79	4.77	21.49	5.49	19.66
12	4.04	27.03	4.94	24.15	5.43	22.82	6.20	20.86
13	4.61	28.45	5.58	25.50	6.10	24.14	6.92	22.23
14	5.20	29.85	6.23	26.84	6.78	25.45	7.65	23.49
15	5.79	31.24	6.89	28.16	7.48	26.74	8.40	24.74
16	6.41	32.62	7.57	29.48	8.18	28.03	9.15	25.99
17	7.03	33.99	8.25	30.79	8.89	29.31	9.90	27.22
18	7.66	35.35	8.94	32.09	9.62	30.58	10.67	28.45
19	8.31	36.70	9.64	33.38	10.35	31.85	11.44	29.67
20	8.96	38.04	10.35	34.67	11.08	33.10	12.22	30.89
21	9.62	39.37	11.07	35.95	11.83	34.35	13.00	32.10
22	10.29	40.70	11.79	37.22	12.57	35.60	13.79	33.31
23	10.96	42.02	12.52	38.48	13.33	36.84	14.58	34.51
24	11.65	43.33	13.26	39.74	14.09	38.08	15.38	35.71
25	12.34	44.64	14.00	41.00	14.85	39.31	16.18	36.90

a. The lower bound is calculated so that  $\beta$  is less than the indicated value.

TABLE 4 (Concluded)

Confidence Interval	90.0 Percent		80.0 Percent		70.0 Percent		50.0 Percent	
	$\beta$ 0.050		0.100		0.15		0.25	
Events, $x_0$	Lower Bound	Upper Bound	Lower Bound	Upper Bound	Lower Bound	Upper Bound	Lower Bound	Upper Bound
0	0	3.00	0	2.30	0	1.90	0	1.39
1	0.051	4.74	0.105	3.89	0.16	3.37	0.29	2.89
2	0.36	6.30	0.53	5.32	0.68	4.72	0.96	3.92
3	0.82	7.73	1.10	6.68	1.33	6.01	1.73	5.11
4	1.37	9.15	1.74	7.99	2.04	7.27	2.54	6.27
5	1.97	10.51	2.43	9.27	2.79	8.49	3.37	7.42
6	2.61	11.84	3.15	10.53	3.56	9.70	4.22	8.56
7	3.29	13.15	3.89	11.77	4.35	10.90	5.08	9.68
8	3.98	14.43	4.66	12.99	5.15	12.09	5.96	10.80
9	4.70	15.71	5.43	14.21	5.97	13.25	6.84	11.91
10	5.43	16.96	6.22	15.41	6.80	14.41	7.72	13.02
11	6.17	18.21	7.02	16.60	7.64	15.57	8.62	14.12
12	6.92	19.44	7.83	17.78	8.48	16.71	9.52	15.22
13	7.69	20.67	8.65	18.96	9.34	17.86	10.42	16.31
14	8.46	21.89	9.47	20.13	10.19	19.00	11.33	17.40
15	9.25	23.10	10.30	21.29	11.06	20.13	12.24	18.49
16	10.04	24.30	11.14	22.45	11.92	21.26	13.15	19.57
17	10.83	25.50	11.98	23.61	12.79	22.38	14.07	20.65
18	11.63	26.69	12.82	24.76	13.67	23.50	14.99	21.73
19	12.44	27.88	13.67	25.90	14.55	24.62	15.91	22.81
20	13.25	29.06	14.53	27.05	15.43	25.74	16.83	23.88
21	14.07	30.24	15.39	28.19	16.31	26.85	17.75	24.96
22	14.89	31.41	16.24	29.32	17.20	27.96	18.68	26.03
23	15.72	32.59	17.11	30.45	18.09	29.07	19.61	27.10
24	16.55	33.75	17.97	31.58	18.98	30.17	20.54	28.17
25	17.38	34.92	18.84	32.71	19.88	31.26	21.47	29.23

Even though we have obtained confidence bounds on the estimate of  $m = \lambda t$ , the major interest is concerned with the upper bounds that an investigator should use when only  $x_0$  events have been observed over a " $t$ " week time interval. Following this concept and the simple model of a large dose-event-week, we recall that only 3 such event weeks occurred over the 300 active weeks of the 19th solar cycle. Now if one wishes to find the upper bounds on this observation, he may use Table 4 in conjunction with Table 3 and arrive at the 100% confidence level that the probability is no greater than some small value  $\alpha$  that  $N_\alpha$  events will occur. Thus Table 5 is

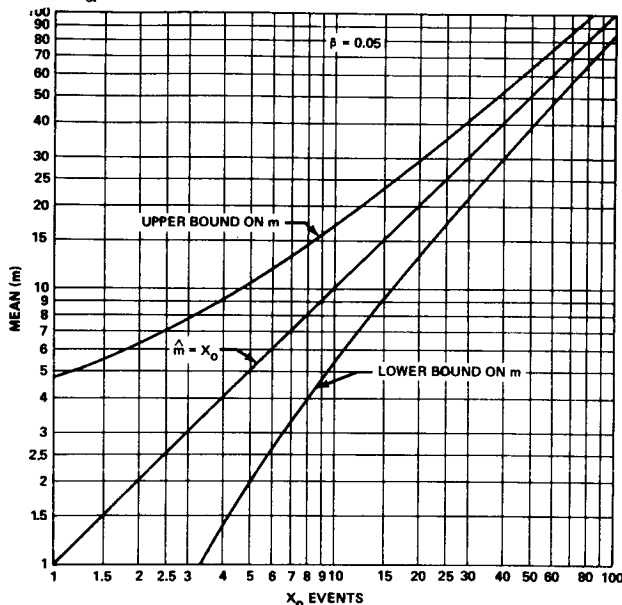


FIGURE 3: 90% CONFIDENCE LIMITS FOR POISSON

TABLE 5: THE NUMBER OF EVENTS  $N_\alpha$  THAT WILL BE EXCEEDED AT A PROBABILITY NO GREATER THAN  $\alpha$  FOR THE 100-PERCENT UPPER BOUND VALUE OF THE POISSON MEAN,  $m'$ , WHEN  $X_0 = 3$  OBSERVED EVENTS

$m'$	$\alpha$									
	100P Percent	0.001	0.005	0.010	0.025	0.050	0.100	0.150	0.250	0.500
13.06	99.9	25	23	22	20	19	18	17	15	13
10.98	99.5	22	20	19	18	17	15	14	13	11
10.05	99.0	21	19	18	17	15	14	13	12	10
8.77	97.5	19	17	16	15	14	13	12	11	9
7.75	95.0	18	16	15	14	13	11	11	9	8
6.68	90.0	16	14	13	12	11	10	9	8	7
6.01	85.0	15	13	12	11	10	9	8	7	6
5.11	75.0	13	12	11	10	9	8	7	6	5
3.67	50.0	11	9	9	8	7	6	6	5	3

a. Example: One is 95 percent confident that the true mean does not exceed 7.75 ( $X_0=3$ ), and using this value of the mean, one is certain that the probability of seeing more than 13 events during a 300 week active period is no greater than 0.050.

TABLE 6: THE NUMBER OF EVENTS  $N_\alpha$  THAT WILL BE EXCEEDED AT A PROBABILITY NO GREATER THAN  $\alpha$  FOR THE 100P-PERCENT UPPER BOUND VALUE OF THE POISSON MEAN,  $m'$ , WHEN  $X_0 = 0$  OBSERVED EVENTS

$m'$	$\alpha$									
	100P Percent	0.001	0.005	0.010	0.025	0.050	0.100	0.150	0.250	0.500
6.91	99.9	16	15	14	12	11	10	10	9	7
5.30	99.5	14	12	11	10	9	8	8	7	5
4.61	99.0	12	11	10	9	8	7	7	6	4
3.69	97.5	11	9	9	8	7	6	6	5	4
3.00	95.0	10	8	8	7	6	5	5	4	3
2.30	90.0	8	7	6	6	5	4	4	3	2
1.90	85.0	7	6	6	5	4	4	3	3	2
1.39	75.0	6	5	5	4	4	3	3	2	1
0.69	50.0	4	4	3	3	2	2	2	1	0

constructed.

Since the 20th solar cycle has produced no large events, it is of interest to ask if zero large events occur for a period of 300 active weeks, what are the possible upper bounds of  $m'$  and the number of events  $N_{\alpha}'$  that could be expected at some small probability. (This may be a nonsense question and will be discussed in the next section.) Table 6 is constructed with this in mind. The methods used are the same as for Table 5. It is of interest to note that even though  $x_0 = 0$  events are observed that the 95% upper bound for the Poisson mean is  $m' = 3$  which was the actual observed number of large events during the 19th cycle. Thus it seems that for a reasonable level of confidence (95%), the analyst would be justified if he used  $m' = 3$  ( $\lambda = 0.01$  event/week) for large events even though the solar activity for a given cycle was considerably different than the 19th cycle. Perhaps after all is said, the only conclusion that can be drawn is that the observed 19th cycle dose events could be used for any near average solar cycle, and if a cycle is predicted to be similar to the 19th cycle, then the results of Table 5 ( $x_0 = 3$ ) should be seriously considered as a possible model.

Finally, Table 7 is presented as a summary of values to use for  $\lambda$  (events/week) at various confidence levels. For large events, it seems that the  $x_0 = 0$  column is probably reasonable to use if the solar cycle is not very active. If a cycle similar to the 19th is forecast, then the column under  $x_0 = 3$  is preferred.

TABLE 7: VALUES FOR  $\lambda' = m'/300$  (EVENTS/WEEK) FOR  $X_0$  OBSERVED EVENTS AT 100% UPPERBOUND CONFIDENCE LEVEL

$X_0$ 100PZ	0	3	6	9
99.9	.0230	.0435	.0602	.0755
99.5	.0177	.0366	.0522	.0667
99.0	.0154	.0335	.0486	.0626
97.5	.0123	.0292	.0435	.0569
95.0	.0100	.0258	.0393	.0524
90.0	.0070	.0223	.0351	.0474
85.0	.0063	.0200	.0323	.0442
75.0	.0046	.0170	.0285	.0392
50.0	.0023	.0122	.0222	.0322
OBS*	.0000	.0100	.0200	.0300

\*OBS denotes the value of  $X_0/300$

The value of  $\lambda$  and the dose event model to use during the remaining 270 less active weeks of a solar cycle are not obtainable from the present analysis. However, until more data is available, the best one can do is use some essentially arbitrary criteria. For example, if we believe that the chance of a large dose event week is definitely dependent on some minimal level of solar activity and this level is not approached during the quiet periods of the cycle, then it would be unreasonable to use the large event dose week even at a very low probability level such as the values shown under the  $x_0 = 0$  column of Table 7. Even if  $\lambda$  is only .002 event/week for the Poisson distribution, one sees that the chance of getting two or more large events is approximately 6% for  $t = 200$  weeks. However, we cannot preclude the possibility of some smaller dose event occurring for the quiet period of a solar cycle. The present writer suggests using  $\lambda = .02$  event/week for the quiet period but recommends that the dose model for the small dose event ( $D_3$ ) of Model II (Table 2) be used. This is equivalent to expecting about one such event per year which is reasonably close to the actual observed number of events from October 1961 through July 1966.

In order to illustrate applications of the foregoing work, eight trip lengths will be considered ranging from 13 to 260 weeks (5 years), during the most active 6 years of a solar cycle which is like the 19th cycle ( $x_0 = 3$ ). In order to simplify the possible combinations, four different probability levels for the upper bound mean ( $\lambda$ ) are used at four probability levels for the Poisson distribution. A mean (.01 t) corresponding to the actual observed (OBS) large event weeks of the 19th cycle is also given. This corresponds to the 95% level of the mean for  $x_0 = 0$  events, and this value is recommended for the average type cycle. The results of these combinations are shown in Table 8. The entries in this table give the number of large events that will be expected at a probability equal to or less than  $\alpha$  corresponding to the Poisson mean ( $\lambda t$ ) which we are 100% sure will not be exceeded (see footnote on Table 5). These tables are constructed in a manner similar to Table 5, however, we start with Table 7 for values of  $\lambda$  at various levels of percent confidence (100P).

Figures 4, 5, and 6 have been presented for values of  $\alpha$  at .001, .01, and 0.1 for different upper bound values of the mean showing a range from the observed (approximately 50%) to the 99.9% confidence level of the mean ( $\lambda t$ ) for a 78-week mission during the active weeks of a very active cycle. Comparisons are also shown in these figures to the work of other authors<sup>[2,9,10]</sup> who have made similar computations but have used different models for prediction of the solar proton dose. An interesting aspect of the above comparison is that at the 0.1% ( $100 \alpha$ ) level, the present work is considerably lower even for the 99.9% upper bound value of  $\lambda t$ . However, at the 10% level, the reverse situation seems to be the case. The major difference in the methods of most of the other authors and the present work is that the size of our large event is fixed, but the number of events may be quite large, whereas in the other methods, the size of a single event may be extremely large (several times larger than the large event used in this work). These differences will be discussed in the last section.



TABLE 8: NUMBER OF EVENTS AT COMPOUND PROBABILITIES P AND  $\alpha$

a. t = 13 Weeks					e. t = 104 Weeks								
m = $\lambda t$	P $\times$ 100	$\alpha$	0.001	0.01	0.05	0.10	m = $\lambda t$	P $\times$ 100	$\alpha$	0.001	0.01	0.05	0.10
0.57	99.9	4	3	2	2	2	4.52	99.9	12	10	8	7	7
0.44	99.0	3	2	2	1	1	3.48	99.0	10	8	7	6	6
0.34	95.0	2	2	1	1	1	2.68	95.0	9	7	6	5	5
0.29	90.0	2	2	1	1	1	2.32	90.0	9	6	5	4	4
0.13	OBS	1	1	1	1	1	1.04	OBS	5	4	3	2	2

b. t = 26 Weeks					f. t = 156 Weeks								
m = $\lambda t$	P $\times$ 100	$\alpha$	0.001	0.01	0.05	0.10	m = $\lambda t$	P $\times$ 100	$\alpha$	0.001	0.01	0.05	0.10
1.13	99.9	6	4	3	3	3	6.79	99.9	16	16	11	10	10
0.87	99.0	5	4	3	2	2	5.23	99.0	14	11	9	8	8
0.67	95.0	4	3	2	2	2	4.02	95.0	11	9	8	7	7
0.58	90.0	4	3	2	2	2	3.48	90.0	10	8	7	6	6
0.26	OBS	3	2	1	1	1	1.56	OBS	7	5	4	3	3

c. t = 52 Weeks					g. t = 208 Weeks								
m = $\lambda t$	P $\times$ 100	$\alpha$	0.001	0.01	0.05	0.10	m = $\lambda t$	P $\times$ 100	$\alpha$	0.001	0.01	0.05	0.10
2.26	99.9	8	6	5	4	4	9.05	99.9	20	17	14	13	13
1.74	99.0	7	5	4	3	3	6.97	99.0	16	14	12	10	10
1.34	95.0	6	5	3	3	3	5.37	95.0	14	11	9	8	8
1.16	90.0	6	4	3	3	3	4.64	90.0	13	10	8	7	7
0.52	OBS	4	3	2	1	1	2.08	OBS	8	6	5	4	4

d. t = 78 Weeks					h. t = 280 Weeks								
m = $\lambda t$	P $\times$ 100	$\alpha$	0.001	0.01	0.05	0.10	m = $\lambda t$	P $\times$ 100	$\alpha$	0.001	0.01	0.05	0.10
3.39	99.9	10	8	7	6	6	11.31	99.9	23	20	17	16	16
2.61	99.0	9	7	5	5	5	8.71	99.0	19	16	14	13	13
2.01	95.0	8	6	5	4	4	6.71	95.0	16	13	11	10	10
1.74	90.0	7	5	4	3	3	5.80	90.0	14	12	10	9	9
0.78	OBS	5	3	2	2	2	2.80	OBS	9	7	5	5	5

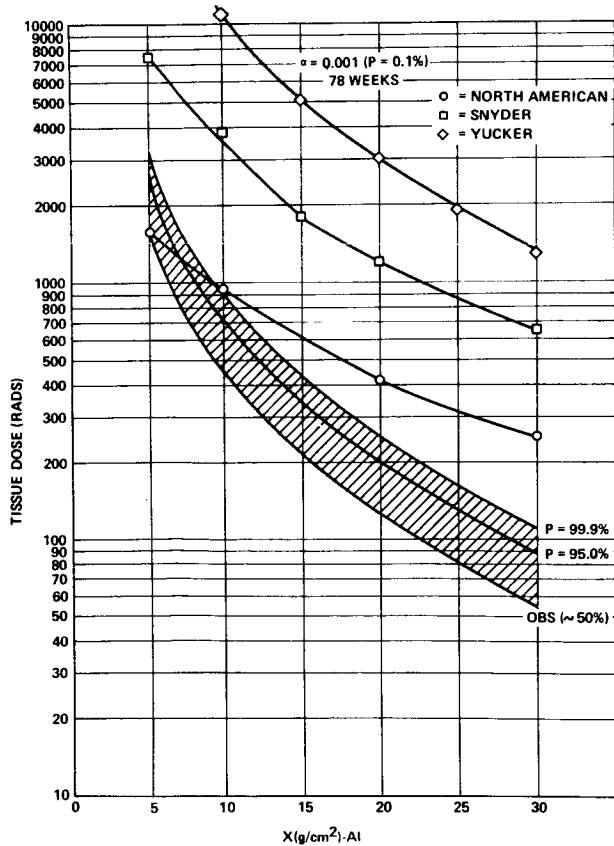


FIGURE 4: DOSE CURVES AT PROBABILITIES  $\alpha = .001$

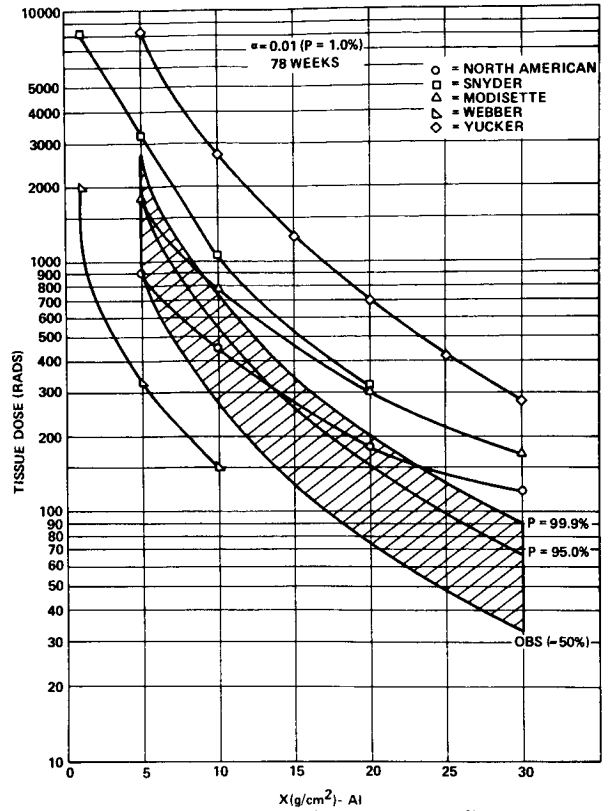


FIGURE 5: DOSE CURVES AT PROBABILITIES  $\alpha = .01$

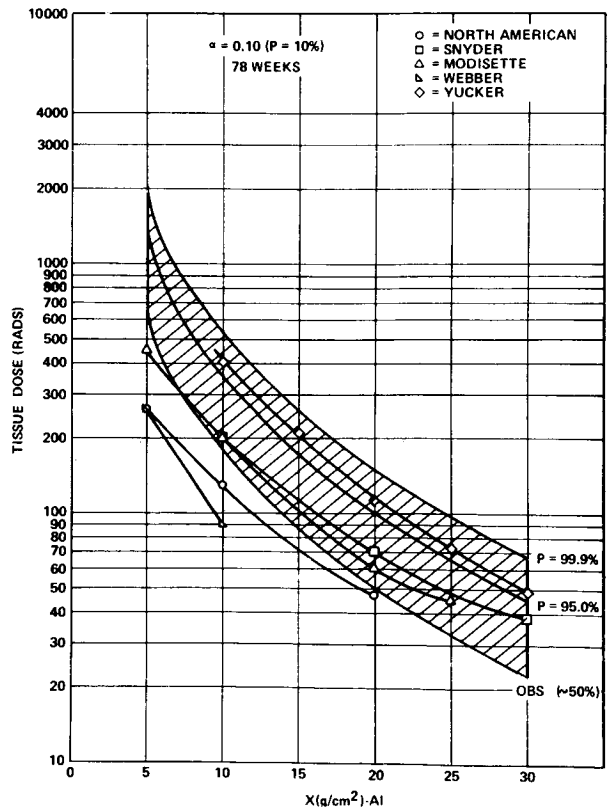


FIGURE 6: DOSE CURVES AT PROBABILITIES  $\alpha = .1$

A NEW PROBABILITY MODEL IS FOUND

The foregoing section seems to provide some rationale for choosing a probability function for a given set of conditions: (a) the active 300 weeks of a very active cycle such as the 19th, (b) the active 300 weeks of an average cycle, and (c) the quiet 270 weeks of any solar cycle. However, if we examine Tables 5 through 8, a question presents itself. If we choose a very high confidence level for the Poisson mean and then determine the number of events that would give a low probability  $\alpha$  of getting a worse situation, then it seems that we are discussing a very improbable situation. That is, what is the chance of the mean being as high as the 99.9% confidence level, and if we use this mean the joint probability of seeing more than  $N_{\alpha}'$  events at a probability no greater than 0.001? For example, in Table 5, we see that  $N_{\alpha}' = 25$  events when  $P = .999$  and  $\alpha = .001$ . At first blush, one might suspect that the chance of both conditions occurring is on the order of  $10^{-6}$ . But care must be taken since we are dealing with cumulative distribution functions. Thus the product  $(1 - P)\alpha$  does not correspond to a unique value of  $N_{\alpha}'$ . This can be ascertained by examining in Table 5 the values of  $(1 - P)\alpha$  corresponding to  $N_{\alpha}' = 13$ . Now, we would like to ask the question;

"If  $x_0$  events are observed in a given time,  $t_0$ , what is the probability of seeing more than  $N$  events in any observation time  $t$ ?"

With this knowledge a unique value of the probability of seeing  $N$  events can be made for any period  $t \leq T_0$ . This question is also important because we propose to use the values of  $\lambda$  calculated for the total period of  $T_0 = 300$  weeks and might be suspect of the true probability when one applies the value of  $\lambda$  to a time period say of only 50 weeks. However, the reader surely agrees that the best estimate of the  $\lambda$  corresponds to the total sample space of the 300 most active weeks during the 19th solar cycle.

In order to provide an answer to the above, we must first ask what is the distribution of possible Poisson means if in a time  $t_0$  there are only  $x_0$  events observed. If we examine Equation (13), which gives the cumulative distribution of  $\beta$  as a function of the upper bound values of  $m$  for a given  $x_0$ , one sees that the derivative  $(-d\beta/dm)$  yields the desired upper bound probability density function for  $m$ ;

$$-d\beta/dm = f(m) = \frac{e^{-m} m^{x_0}}{x_0!} \quad (16)$$

This function is continuous in  $m$  and is the so-called gamma distribution in the variate  $m$ . The expected value of  $m$ ,  $E(m) = x_0 + 1$ ; the variance,  $\sigma^2(m) = x_0 + 1$ , and

$$\int_0^{\infty} \frac{e^{-m} m^{x_0}}{x_0!} dm = 1 \quad (17)$$

To summarize the meaning of Equation (16), we can state that for a given observation of  $x_0$  events, the probability of the  $m$  being in the interval  $m$  to  $m + dm$  is given by the probability equation;

$$f(m)dm = \frac{e^{-m} m^{x_0}}{x_0!} dm \quad (18)$$

See Fig. 7 for illustration of Equation (18) with  $x_0 = 3$ .

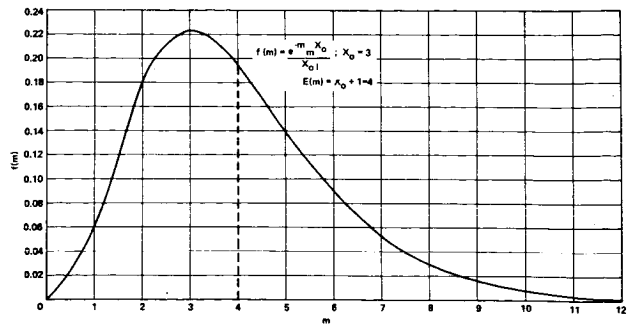


FIGURE 7: THE GAMMA PROBABILITY DENSITY FUNCTION WHEN  $x_0 = 3$

However, we wish to investigate the more subtle relationship that reflects the distribution of  $\lambda$ 's for a given observation of  $x_0$  events over a period of  $t_0$  weeks. Therefore, we make the change of variables denoted by  $m = \lambda t_0$ ;  $dm = t_0 d\lambda$ , and our probability density function in the variate  $\lambda$  becomes:

$$f(\lambda)d\lambda = \frac{t_0^{x_0+1}}{x_0!} \lambda^{x_0} e^{-\lambda t_0} d\lambda \quad (19)$$

For a given value of  $\lambda$ , the probability of seeing exactly  $x$  events in time " $t$ " is given by the discrete Poisson distribution function;

$$P(x) = \Pr(x; \lambda t) = \frac{(\lambda t)^x e^{-\lambda t}}{x!}, \quad x=0,1,2,\dots \quad (20)$$

where the probability of having a value of  $\lambda$  in the interval  $\lambda + d\lambda$  is given by the density function of Equation (19) and  $t \leq t_0$  (actually the case  $t > t_0$  is equally valid).

Using the above definitions, the relationship we seek is given by the following:

$$\Pr(x, t | x_0, t_0) = \int_0^{\infty} \Pr(x; \lambda t) \cdot f(\lambda) d\lambda \quad (21)$$

Thus we are stating that for Equation (20) of the Poisson distribution, the probability of each possible  $\lambda$  (a spectrum of possible means) be folded into the equation and the results integrated over all possible values of  $\lambda$  from zero to infinity. The result is a probability density function which is the expected value of the Poisson distribution over all possible means  $\lambda$ . Thus,

$$\Pr(x, t | x_0, t_0) = \frac{t_0^{x_0+1} t^x}{x_0! x!} \int_0^{\infty} \lambda^{x_0+x} e^{-(t_0+t)\lambda} d\lambda \quad (22)$$

After integration, we obtain;

$$\Pr(x, t | x_0, t_0) = \frac{t_0^{x_0+1} t^x}{x_0! x!} \left[ \frac{(x_0+x)!}{(t_0+t)^{x_0+x+1}} \right] \quad (23)$$

Now if we make the substitution  $\theta = t/t_0$  and simplify, the results are the discrete distribution function in the variate  $x$ :

$$\Pr(x | x_0, \theta) = \frac{(x+x_0)!}{x! x_0!} \frac{\theta^x}{(1+\theta)^{x+x_0+1}} \quad (24)$$

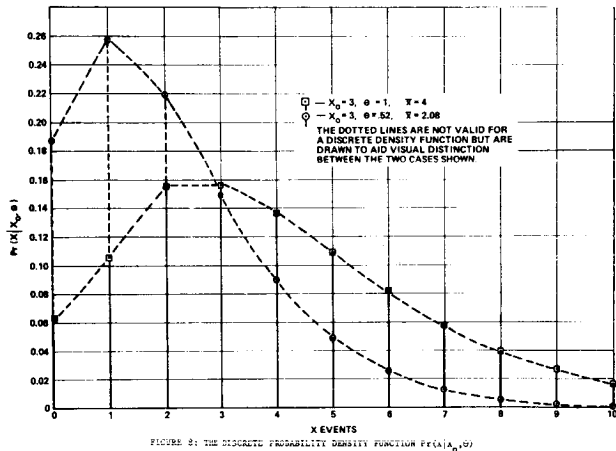
It can be shown that for the discrete distribution function above;

$$\sum_{x=0}^{\infty} \frac{(x+x_0)!}{x!x_0!} \frac{\theta^x}{(1+\theta)^{x+x_0+1}} = 1, \quad (25)$$

and the mean or expected value of  $x$  is given by:

$$\bar{x} = E(x) = (x_0+1)\theta. \quad (26)$$

The proof of Equation (25) can be shown by resorting to hypergeometric functions, and the results of Equation (26) can be found by multiplying the summand of Equation (25) by  $x$  and after simplifying, the value  $(x_0+1)\theta$  can be factored out leaving a sum that is the equivalent to that shown in Equation (25). An illustration of the density function [Equation (24)] is shown in Fig. 8 for  $\theta = 1$  and  $\theta = .52$ .



This report is not intended to be a study of probability theory, and the ramifications of the above distribution function and its possible parallels in other statistical work will not be pursued.

Because of the format of Tables 5 and 8 and the manner in which we have previously made probability statements, we wish to find the probability that more than  $N$  events are seen, given  $x_0$  and  $\theta$ ; or

$$Pr(x > N | x_0, \theta) = 1 - Pr(x \leq N | x_0, \theta), \quad (27)$$

where  $\theta = t/t_0$ ,  $x_0$  = number of events observed in time  $t_0$  (300 weeks), and  $t$  is the observation time during which  $N$  events are seen.

Thus, the ultimate relation which we wish to answer our probability questions is given by Equation (27) or the obvious variations associated with it. In fact, if the foregoing is valid, we may dispense with the difficulties of choosing an upper bound value of the Poisson mean at a given level and then determining the probability that  $N$  events will be exceeded at some probability  $\alpha$  as shown in Tables 5 and 8, where the true probability is actually not known.

Using Equation (27), the number of combinations of  $\theta$ ,  $x_0$ , and  $N$  can readily get out of hand. For this reason, only the values of  $x_0$  observed events from 0 through 9 were used with different values of  $\theta$  from 13 weeks to 300 weeks ( $\theta = 1$ ). The values of  $N$  were extended to the point where  $Pr(x > N | x_0, \theta) < 10^{-6}$ . These tabulations are given in reference 8.

It is very interesting to note that when  $x_0 = 0$ ,  $\theta = 1$ , that the chance of seeing more than 3 events is as high as .0625. This infers that even though no events were observed during a given 300 week active cycle, we cannot be more than 93.75% confident that 3 or less events could occur in a similar cycle. Also, we see from the same above assumption that we are 50% sure that we will see more than zero events. This seems to infer a dilemma bordering on the naive statement that if you know nothing about the probability of an event, you can only be 50% sure that it can't happen; e.g. probability of life on Mars. This last statement seems to cast doubt on the usefulness of the case when  $x_0 = 0$ .

However, it is of academic interest to investigate further the case when  $x_0 = 0$ . For example, Equation (24) becomes:

$$Pr(x | 0, \theta) = \theta^x / (1+\theta)^{x+1} \quad (28)$$

and for  $\theta > 0$ , we see that when  $x = 0$ ,

$$Pr(x = 0 | 0, \theta) = 1 / (1 + \theta), \quad (29)$$

and

$$Pr(x > 0 | 0, \theta) = \theta / (1 + \theta). \quad (30)$$

The probability of seeing an event as  $\theta$  approaches zero becomes very small as one would suspect for a very rare event. Now as  $\theta$  increases to large values ( $\theta \gg 1$ ), the value of the probability approaches 1. This infers that if an event can happen at a given small probability, then it is almost certain that the event will occur after a sufficiently long period. Thus Equations (29) and (30) do not defy intuition in an ordinary sense but leave us with a rather insecure feeling since the number of actual observed events in time  $t_0$  is zero. However, if we examine the density function of possible values of  $\lambda$  [Equation (19)] when  $x_0 = 0$ , a plausible probability density function is found;

$$f(\lambda) d\lambda = t_0 e^{-t_0 \lambda} d\lambda. \quad (31)$$

Table 9 is presented as a survey of Equation (27) for  $Pr(x > N | 3, \theta) \leq \epsilon$  at several values of  $\epsilon$  and  $\theta$ .

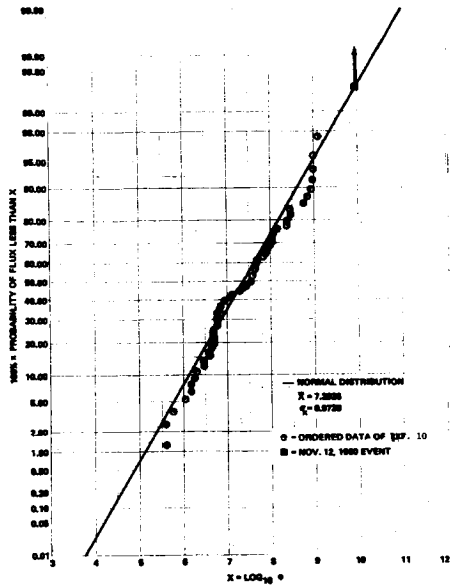


FIGURE 9: CUMULATIVE DISTRIBUTION OF LOG FLUX FOR 19TH CYCLE

A point of interest concerns the values of the results in Table 8 as compared to those in Table 9. It should be clear that the results of Table 9 do not provide the same type of probability statements as Table 8. In general, this writer feels that the results of Table 9 are more useful and to the point but others may disagree. In any case, one may ascertain which probability level of the parameter  $\lambda$  is more credible when using the methods of the previous section and constructing tables similar to Table 8. For example, one sees that the value of  $\lambda$  at the 90% level seems to yield event numbers (N) at probabilities  $\alpha$  in Table 8 which seem to be comparable to the probabilities  $\epsilon$  in Table 9.

Finally Table 10 is presented for the case when  $x_0 = 0$  even though we have cast doubt on the validity of the meaning of this rather extreme case. However, it does signify a sort of boundary condition for those periods when the probability of a large event is very small as perhaps exists for the active years of an average type solar cycle.

#### REVIEW AND COMMENTS

In the foregoing sections, the writer has attempted to convey a method of thinking about the radiation hazards associated with solar proton events. The method of approach is felt to be more important than the actual results presented. The methods and models as developed utilize very little solar physics as such and consequently will be very unsatisfying to many physicists who have examined various aspects of the problem. There is no attempt to model or predict a solar proton spectrum, the time dependence of particle arrival, or angular distributions of the flux.

As a brief summary, the total dose in rads-tissue from solar protons was tabulated for weekly time intervals, and the number of weeks which gave a dose above 25 rads behind 10 g/cm<sup>2</sup> of aluminum for the active 6 years of the 19th cycle were called dangerous or large event weeks. The number of such event weeks was found to be only 3 weeks for the past 20 years.

Even though the chance for smaller events is examined, it was found that for any reasonable high confidence level (95%), the smaller events could be ignored. Consequently, we took the total particle flux for the 19th cycle and divided this spectrum by a factor of 3 and arrived at a single large event week.

Using this spectrum, one can calculate the tissue dose in rads at the center of an aluminum spherical shell (Table 2). To correct for geometric effects and self shielding, this dose should be reduced by a factor of about 3. If the space mission is planned during the quiet period of a cycle, then the small event dose curve (D<sub>3</sub>) of Model II (Table 2) may be used with  $\lambda = .02$  ( $\mu \approx 1$  event/year).

To predict the probability of an event occurring, the Poisson distribution seemed to be the most logical choice. The third section was devoted to examining this conclusion and the methods of using this probability model. The fourth section was written as an effort to define the confidence one could use in employing the Poisson process and specifically arriving at confidence levels for the experimental or observed value of the mean of the Poisson distribution function. Several examples were given for different mission lengths, and comparisons were made to other authors' results.

Finally, the previous section was an extension of the Poisson process to incorporate the concept of small sample theory and arrive at the expected distribution function which answers the following question. If  $x_0$  events are observed in time  $t_0$ , what is the probability of seeing  $x$  events in any observation time  $t$ ? The results were represented by the discrete probability density function in the variate  $x$ :  $\text{Pr}(x|x_0, t_0)$ . Using the above function, extensive tables were tabulated in reference 8.

In the beginning of this work, the author intended to avoid commenting on the methods used by other investigators, but in order to explain the radical differences shown in Figs. 4, 5, 6, the following comments are pertinent. One of the more common procedures used is to obtain the logarithms to the base ten of the solar proton flux above 30 MeV for each of the events of the 19th cycle. This data is then plotted on normal probability graph paper, obtaining a distribution called the log normal distribution in the variable  $x = \log_{10} \phi$ .

This is a true normal distribution in the variate  $x$ , and there is no virtue in examining the transformed distribution in the variable  $\phi$  which has a more complex representation. Also the values of the mean and standard deviation between the two distributions are not simply antilog related. For more details, see reference 8.

The present writer has assumed that the users of this distribution keep their statistics in the variable  $x$  which is certainly the simplest process.

From reference 10, 60 events were taken that had fluxes measured above 30 MeV.

The logarithm of these 60 entries were ordered from the smallest to the largest and the normalized cumulative sums plotted on log normal paper as shown in Fig. 9. The ungrouped data had a mean of 7.39, and the standard deviation was 0.97 as shown at bottom of the figure. The straight line in Fig. 9 depicts the cumulative normal distribution

TABLE 9: NUMBER OF EVENTS N THAT SATISFY  $\Pr(X > N | 3, \theta) \leq \epsilon$ 

WEEKS	$\epsilon$					
	$\theta$	.10	.01	.001	.0001	.00001
13	.0433	1	2	3	3	4
26	.0866	1	2	4	5	6
52	.1733	2	4	5	7	8
78	.2600	3	5	7	8	10
104	.3467	3	6	8	10	12
156	.5200	4	8	10	13	16
208	.6933	6	9	13	16	19
260	.8667	7	11	15	19	22
300	1.000	9	13	17	21	25

with mean of 7.39 and variance of 0.97. From examination of this fit, one might conclude that the log normal gives a reasonable representation of the data. Note that the flux for the November 12, 1960, event is plotted as a square which falls exactly on our line of best fit. This is done since actually when one obtains the cumulative distribution from a discrete set of data, the last point has the cumulative probability of 1.00, but since this cannot theoretically occur, the best choice is to place this point on the best fit line. This point which is  $\log_{10} \phi = 9.9562$  corresponds to the cumulative probability of 99.6% or in terms of the standard deviation, the November 12, 1960, event is at 2.63 standard deviations above the mean. If we wished to go to the 99.9% level, then it would be necessary to take 3.09 standard deviations above the mean or a log flux of 10.4016. Now if we find the antilog of this value, we see that the flux at the 99.9% level in the log normal distribution is  $2.52 \times 10^{10}$  proton/cm<sup>2</sup> ( $E > 30$  MeV) which is a factor of about 2.8 times larger than the November 12, 1960, event. Hence, it would seem that a flux above 30 MeV which is 3 times larger than the November 12, 1960, event would have a probability of occurring which is less than 0.001.

From the above analysis, one may be convinced that a reasonable upper bound value for a single event is at most a factor of 3 larger than the November 12, 1960, event. For the above reason this writer feels that the results obtained by some investigators for the extreme probability tails must depict a smaller probability than the estimates given. They have possibly used joint probabilities of flux and rigidity parameters which may be a factor of 10 or more smaller than those indicated by the 0.1% probability tail shown in the various reports at my disposal.

If the reader wishes to use the 99.9% probability event in the present work, he may ignore self shielding and geometry factors, a factor of 3.

TABLE 10: NUMBER OF EVENTS N THAT SATISFY  $\Pr(X > N | 0, \theta) \leq \epsilon$ 

t WEEKS	$\epsilon$					
	$\theta$	.1	.01	.001	.0001	.00001
13	.0433	0	1	2	2	3
26	.0866	0	1	2	3	4
52	.1733	1	2	3	4	6
78	.2600	1	2	4	5	7
104	.3467	1	3	5	6	8
156	.5200	2	4	6	8	10
208	.6933	2	5	7	10	12
260	.8667	2	5	8	11	14
300	1.0000	3	6	9	13	16

## REFERENCES

1. WEDDELL, J.B.; and HAFNER, J.W.: Statistical Evaluation of Proton Radiation from Solar Proton Events. North American Aviation, SID 66-421, May 1966.
2. FRENCH, F.W.: Solar Flare Radiation Protection Requirements for Passive and Active Shields. AIAA 7th Aerospace Sciences Meeting, Paper No. 69-15, January 1969.
3. BURRELL, M.O.; WRIGHT, J.J.; and WATTS, J.W.: An Analysis of Energetic Space Radiation and Dose Rates. NASA TN D-4404, February 1968.
4. MASLEY, A.J.; and GEODEKE, A.D.: A Complete Dose Analysis of the November 12, 1960, Solar Cosmic Ray Event. Life Sciences and Research, 1963.
5. WEBBER, W.R.: An Evaluation of the Radiation Hazard Due to Solar Particle Events. Boeing Document D2-90469, December 1963.
6. WHITE, T.T.; ROBBINS, D.E.; and HARDY, A.C.: Radiation Environment for the 1975 - 1985 Space Station Program. MSC Document MSC-00183, October 1969.
7. FELLER, W.: An Introduction to Probability Theory and Its Application. Vol. I, 1957.
8. BURRELL, M.O.: The Risk of Solar Proton Events to Space Travel. NASA TN D (to be published in early 1971).
9. SNYDER, J.W.: Radiation Hazard to Man From Solar Proton Events. J.Sci. Res., Vol. 4, 1967, p. 826.
10. YUCKER, W.R.: Statistical Analysis of Solar Cosmic Ray Proton Dose. McDonald Douglas Report MDC G-0363, June 1970.

#### REFERENCES

1. WEDDELL, J. B.; and HAFFNER, J. W.: Statistical Evaluation of Proton Radiation From Solar Proton Events. North American Aviation, SID 66-421, May 1966.
2. FRENCH, F. W.: Solar Flare Radiation Protection Requirements for Passive and Active Shields. AIAA 7th Aerospace Sciences Meeting, Paper No. 69-15, January 1969.
3. BURRELL, M. O.; WRIGHT, J. J.; and WATTS, J. W.: An Analysis of Energetic Space Radiation and Dose Rates. NASA TN D-4404, February 1968.
4. MASLEY, A. J.; and GOEDEKE, A. D.: A Complete Dose Analysis of the November 12, 1960, Solar Cosmic Ray Event. Life Sciences and Research, 1963.
5. WEBBER, W. R.: An Evaluation of the Radiation Hazard Due to Solar Particle Events. Boeing Document D2-90469, December 1963.
6. WHITE, T. T.; ROBBINS, D. E.; and HARDY, A. C.: Radiation Environment for the 1975 - 1985 Space Station Program. MSC Document MSC-00183, October 1969.
7. FELLER, W.: An Introduction to Probability Theory and Its Applications. vol. I, 1957.
8. BURRELL, M. O.: The Risk of Solar Proton Events to Space Travel. NASA TN D (to be published in early 1971).
9. SNYDER, J. W.: Radiation Hazard to Man From Solar Proton Events. J. Sci. Res., vol. 4, 1967, p. 826.
10. YUCKER, W. R.: Statistical Analysis of Solar Cosmic Ray Proton Dose. McDonald Douglas Report MDC G-0363, June 1970.